Ann. Geophys., 35, 493–503, 2017
www.ann-geophys.net/35/493/2017/
doi:10.5194/angeo-35-493-2017

Annales Geophysicae Open Access EGU

Variations in energy, flux, and brightness of pulsating aurora measured at high time resolution

Hanna Dahlgren[1,2], **Betty S. Lanchester**[2], **Nickolay Ivchenko**[1], **and Daniel K. Whiter**[2]

[1]School of Electrical Engineering, Royal Institute of Technology KTH, Stockholm, Sweden
[2]School of Physics and Astronomy, University of Southampton, Southampton, UK

Correspondence to: Hanna Dahlgren (hannad@kth.se)

Received: 20 January 2017 – Revised: 7 March 2017 – Accepted: 8 March 2017 – Published: 28 March 2017

Abstract. High-resolution multispectral optical and incoherent scatter radar data are used to study the variability of pulsating aurora. Two events have been analysed, and the data combined with electron transport and ion chemistry modelling provide estimates of the energy and energy flux during both the ON and OFF periods of the pulsations. Both the energy and energy flux are found to be reduced during each OFF period compared with the ON period, and the estimates indicate that it is the number flux of foremost higher-energy electrons that is reduced. The energies are found never to drop below a few kilo-electronvolts during the OFF periods for these events. The high-resolution optical data show the occurrence of dips in brightness below the diffuse background level immediately after the ON period has ended. Each dip lasts for about a second, with a reduction in brightness of up to 70 % before the intensity increases to a steady background level again. A different kind of variation is also detected in the OFF period emissions during the second event, where a slower decrease in the background diffuse emission is seen with its brightness minimum just before the ON period, for a series of pulsations. Since the dips in the emission level during OFF are dependent on the switching between ON and OFF, this could indicate a common mechanism for the precipitation during the ON and OFF phases. A statistical analysis of brightness rise, fall, and ON times for the pulsations is also performed. It is found that the pulsations are often asymmetric, with either a slower increase of brightness or a slower fall.

Keywords. Ionosphere (auroral ionosphere; particle precipitation) – magnetospheric physics (magnetosphere–ionosphere interactions)

1 Introduction

The slow ON–OFF blinking of auroral brightness known as pulsating aurora is extremely common in the magnetic midnight to morning hours. The variations are quasiperiodic and are often localised into pulsating patches that are a few tens to hundreds of kilometres wide, and the pulsation periods are typically a few seconds to a few tens of seconds (Johnstone, 1978). The emissions are weak compared with breakup aurora, with N_2^+ 1NG brightness measured at 427.8 nm never exceeding 10 kR, and they are often superimposed on a diffuse background (Royrvik and Davis, 1977). The intensity signature is non-sinusoidal, with fast increase and fall times compared with the ON and OFF periods.

Auroral pulsations are long-lasting events; studies show that they can last for more than 15 h (Jones et al., 2013). Thus, they constitute a significant amount of energy transfer from the magnetosphere to the ionosphere. Rocket and satellite measurements have shown that pulsating aurora is the result of modulated electron fluxes with energies from a few to several tens of kilo-electronvolts (e.g. Bryant et al., 1975; Sandahl et al., 1980; McEwen et al., 1981; Samara et al., 2010). Sandahl et al. (1980) and McEwen et al. (1981) found that the electron precipitation during pulsation minima had a lower mean energy than the precipitation during pulsation maxima. Quantifying the energy flux in auroral pulsations gives a measurement of the energy transfer from the magnetosphere to the ionosphere during these long-lasting and ubiquitous events.

Pulsating aurora has received an increased interest in recent years as there still remain unsolved issues regarding its characteristics and formation (Lessard, 2013). There are several mechanisms proposed to explain the increased particle precipitation during pulsating aurora. The most accepted the-

ory is that high-energy electrons in the central plasma sheet get pitch angle scattered into the loss cone by cyclotron resonance with very-low-frequency (VLF) plasma waves (Coroniti and Kennel, 1970; Johnstone, 1983; Davidson, 1990). Time-of-flight analysis of the energy dispersion of the precipitating electrons as measured by the Reimei satellite showed that the source region of the scattered electrons is near the magnetic equator (Miyoshi et al., 2010). There are two main wave modes that can resonate with plasma sheet electrons in the equatorial plane in the energy ranges observed for pulsating aurora: electrostatic electron cyclotron harmonic (ECH) waves, which will interact with plasma sheet electrons of energies ranging from a few hundred electron volts to a few kilo-electronvolts, and electromagnetic whistler-mode chorus waves, which can resonate with electrons of a few to several tens of kilo-electronvolts (Horne et al., 2003; Meredith et al., 2009). Direct evidence of the correlation between chorus waves measured by the THEMIS spacecraft and ground-based imaging of pulsating aurora was presented by Nishimura et al. (2010) and was further supported by later observations of similar correlations for more events (Nishimura et al., 2011; Jaynes et al., 2013). Anisotropic plasma sheet electrons provide a source of free energy for chorus excitation, and in the interaction process they get scattered into the loss cone. The chorus waves typically appear as repetitive discrete bursts lasting a few seconds, each consisting of multiple chorus elements of rising tone (Trakhtengerts, 1999), giving rise to a superimposed 3 ± 1 Hz modulation. Why wave intensities get modulated in a quasiperiodic manner to form pulsating electron precipitation is still an open question (Li et al., 2013), although a correlation between the chorus wave amplitude and density depletions and enhancements in the equatorial plane has been observed in the THEMIS spacecraft data (Li et al., 2011).

There are also theories where the mechanism is believed to be Fermi-type-acceleration-associated with earthward plasma flow (Nakajima et al., 2012), or where the source region is assumed to be located far from the equatorial magnetosphere, caused by field-aligned potential drops (Sato et al., 2004). Observations of non-conjugate auroral pulsations are difficult to explain with a source mechanism in the equatorial plane, and it seems likely that there can be more than one mechanism to account for pulsating aurora and that the ionosphere can also have an active role in controlling the pulsating pattern (Stenbaek-Nielsen, 1980). The energy input to earth's upper atmosphere is considerable during the commonly occurring pulsating auroral events, and observations, both in the magnetosphere and ionosphere, are crucial to obtain a better understanding of the mechanisms behind the phenomenon.

In this study, we use optical and radar data together with ion chemistry modelling to investigate the change in energy and energy flux during ON and OFF periods, for two events of pulsating aurora. From the high-resolution optical data, the shape and variability of the brightness during the pulsations is studied. We show that sharp reductions in emission brightness can occur during the OFF period, temporally connected with the ON period (either directly after the ON period or directly before). We also present a statistical study of the rise, fall, and ON times of individual pulsations, as well as the occurrence of asymmetric pulsations, where the duration of brightness rise time or fall time is prolonged.

2 Instrumentation

The optical data presented in this work come from the multispectral instrument ASK (Auroral Structure and Kinetics). ASK is an auroral imager, comprising three low-light systems, each with an electron multiplying charge coupled device (EMCCD) detector and individual interference filter for selection of a narrow (~ 1 nm) part of the light spectrum, and a field of view of $3.1° \times 3.1°$. The three imagers are time-synchronised and capture images of the aurora in magnetic zenith at 32 frames per second. For the study here, there are two imagers that are of specific interest, one equipped with a filter centred at 673.0 nm, for observations of N_2 (I_{N_2}), and a second imager observing the atomic oxygen line at 777.4 nm (I_O) (Dahlgren et al., 2008). The ratio of these two emissions, I_O / I_{N_2}, is sensitive to the energy of the precipitating electrons, and the data can therefore be used to provide an estimate of the electron energy by comparing the measured ratio with that derived by a combined electron transport and ion chemistry model for different input energies at a specific energy flux (Lanchester and Gustavsson, 2013). For energies above about 1 keV, I_{N_2} is approximately constant with energy, so that variations in the N_2 emission brightness are caused by variations in the energy flux. This emission can thus be used as a proxy for the energy flux of the precipitating electrons.

At the time of these observations, ASK was located at the European Incoherent Scatter Scientific Association (EISCAT) site outside Tromsø, Norway (69.6° N, 19.2° E, $L = 6.2$). The EISCAT ultra-high-frequency (UHF) radar was running an experiment called arc1, which provides measurements of electron density, electron and ion temperatures, and field-aligned ion drifts with 4 s resolution. Data from ASK and EISCAT have been used here to analyse events of pulsating aurora observed over Tromsø, Norway, during the winter 2006–2007.

3 Observations

The data discussed in this study were captured on two different nights, hereafter called events. On 22 October 2006, an auroral substorm onset took place just after 22 UT (00:30 MLT), when the Kp index was 3, and was followed by several hours of auroral pulsations. On 19 January 2007 there was a substorm with onset at 21 UT, which was also followed by several hours of pulsations, with a Kp index of 2.

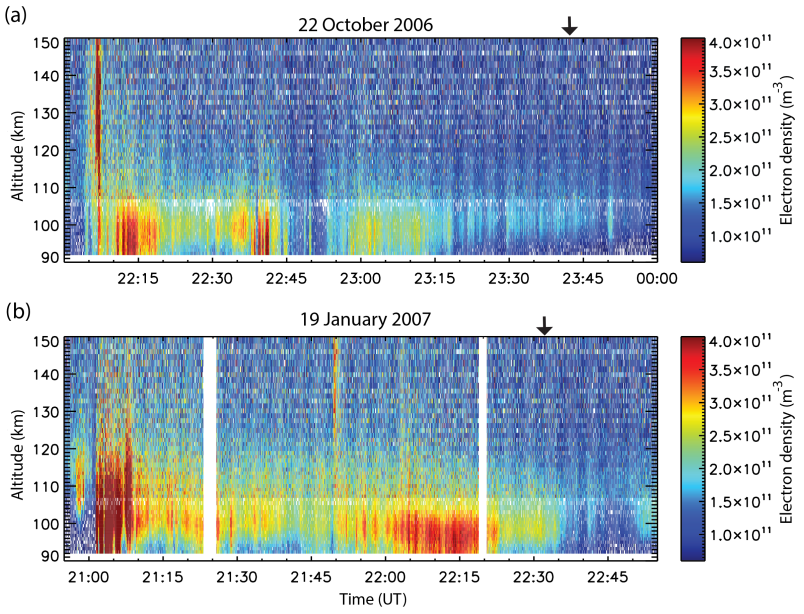

Figure 1. (a) Electron density measurements in magnetic zenith from the Tromsø EISCAT radar on 22 October 2006. The substorm onset at 22:07 UT is seen as the strong ionisation enhancement from 90 km up to above 150 km altitude, and it is followed by 2 h of hard precipitation with ionisation below and at 100 km altitude, during which diffuse pulsations are seen in the optical data. **(b)** Same format as in **(a)**, but for 2 h on 19 January 2007. Substorm onset is at 21:01 UT.

An overview of the ionospheric electron density as a function of time and height measured by EISCAT for 2 h following the onset for both events is shown in Fig. 1. The enhanced ionisation reaches down to well below 100 km altitude on both nights due to high-energy electron precipitation. The optical data showed diffuse emissions with Pc1 pulsations. No 3 Hz modulation was detected in either data set.

3.1 Energy and flux of the precipitation during the pulsations

The pulsations can be seen as E region electron density enhancements in the 4 s resolution EISCAT data. The E region electron density profiles covering a few pulsations between 23:41 and 23:44 UT on 22 October 2006 are displayed in Fig. 2a. I_{N_2} from ASK has been averaged over a circle with 0.1° radius pointed towards the magnetic zenith for each time step and is overplotted as a black trace in the figure. A good correlation between the ON and OFF periods seen in the optical and radar data is found. As expected, there is a slight lag in the radar data due to the cruder temporal resolution and the slow electron recombination rate in the ionosphere (see e.g. Nygrén et al., 1992).

To investigate the temporal evolution of the E region electron density further, the EISCAT data are integrated between 95 and 105 km altitude for each data dump during the time interval in Fig. 2a and plotted in Fig. 2b. The ASK I_{N_2} data are overlaid in red. Five radar dumps during pulsation ON periods were further selected (marked with green diamonds in the plot, and also marked in Fig. 2a at 90 km altitude to indicate the selected radar dumps) and averaged to produce a representative altitude profile. Similarly, five radar data dumps were selected during OFF periods where the electron density data seemed to have reached a minimum value, marked with yellow circles in the plot and below the selected radar dumps in Fig. 2a, to produce an average profile for these OFF periods. The profiles show that both the ON and OFF densities peak near or just above 100 km altitude, which corresponds to electron precipitation with an energy of a few to 10 keV. By using a flux-first fitting algorithm (Palmer, 1995; Lanchester et al., 1998), the measured electron density profiles can be used to estimate the changes in mean energy and energy flux. The radar electron density data, n, together with an assumed recombination rate coefficient, α, lead to an estimated ionisation rate profile q for each time step, through $q = \alpha n^2$, which is plotted as the green data points in Fig. 3a and b for ON and OFF respectively. These are then matched against modelled ionisation rate profiles for the E region, assuming either a monoenergetic (approximated by 10 % half-width Gaussian) or a Maxwellian distribution of the electron spectra, with varying mean energy. Fits are plotted on top of the data profiles in Fig. 3, in red for a Maxwellian distribution and in blue for a monoenergetic distribution. The corresponding mean energies and fluxes of the fits are provided in the legend. Note that fluxes are dependent on the assumed recombination rate coefficient α (here set to 2×10^{-13} m^3 s^{-1}) used to convert electron density profiles to ionisation rate profiles, which affects the absolute flux. It is clear that the

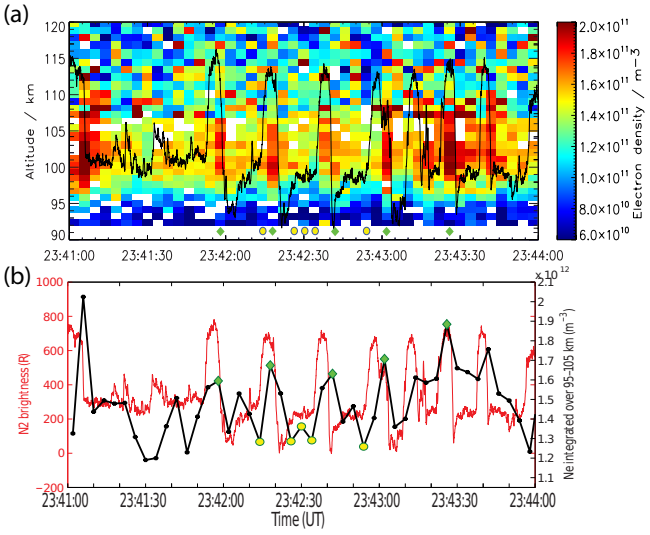

Figure 2. **(a)** Electron density as a function of time and altitude, as measured by EISCAT on 22 October 2006. The pulsations are seen as regular electron density enhancements. I_{N_2} is plotted on top in black. **(b)** Temporal evolution of electron density integrated over 95–105 km altitude (black) and ASK I_{N_2} (red). The green diamonds mark the five data dumps that are averaged to investigate the electron profile during ON, and the yellow circles mark the selected data points to create an average density profile during OFF.

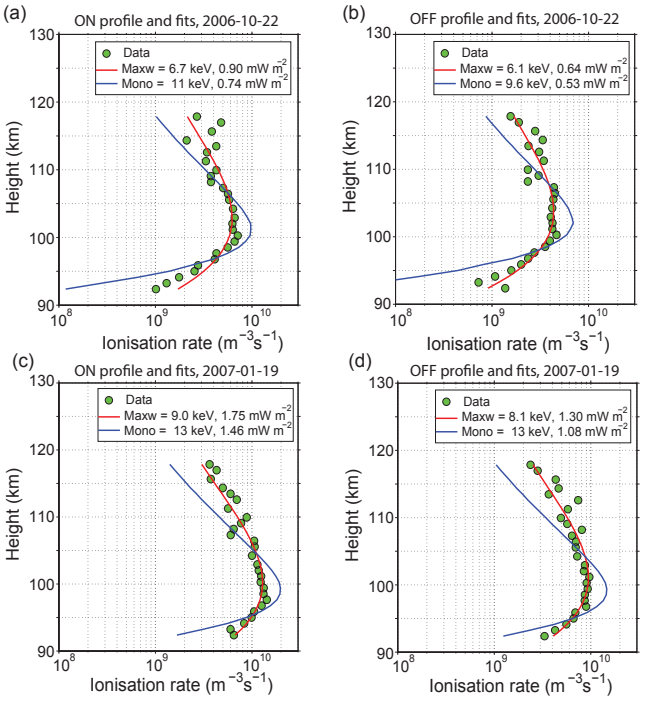

Figure 3. **(a)** Ionisation rate profile from EISCAT electron density data averaged over five measurements during ON periods is shown as green dots from the 2006 event. The line plots are the best fits to the data, as derived with a Maxwellian (red plot) and monoenergetic (blue plot) distribution of the electron spectrum. **(b)** Same as in **(a)**, but for five averaged electron density profiles during OFF periods of the pulsations. **(c)** Same as in **(a)**, but for the 2007 event. **(d)** Same as in **(b)**, but for the 2007 event.

EISCAT data profiles are better fitted with a Maxwellian (red) than a monoenergetic (blue) distribution. The modelled mean energy for the ON period is 6.7 keV, which drops to 6.1 keV during OFF periods, together with a reduction of the energy flux from 0.90 to 0.64 mW m^{-2}. The same analysis was made for the 2007 event; however, here the pulsations had a shorter period, which made the separation between ON and OFF less pronounced in the radar data. Nevertheless, average profiles were produced of five ON and five OFF pulses and the flux-first fitting algorithm was applied. The times of the selected pulsations for both events are marked with arrows on top of each EISCAT spectrum in Fig. 1. Figure 3c shows the result for ON and Fig. 3d for OFF for the 2007 data. Again, a Maxwellian distribution seems more appropriate than a monoenergetic one. Both energies and energy flux are larger than for the 2006 event, with a mean energy of 9.0 keV during ON and 8.1 keV during OFF, and an energy flux reduction from 1.75 to 1.30 mW m^{-2}. On average, the energy decreases by a factor of 9 % for both events, while the energy flux decreases by 27 %. The shapes of the profiles are similar for both events and the main difference between ON and OFF is that the flux is lower during OFF.

The energy and flux have also been investigated using the ASK emission ratio method together with ionospheric modelling, for both events, where the optical data were averaged over a circle with a radius of 0.2° in the magnetic zenith. The I_O and I_{N_2} ratios were compared with modelled emission ratios produced from a catalogue of Maxwellian electron energy profiles for the input electron energy spectra. The radar fits in Fig. 3 make the choice of Maxwellian profiles sensible. For the 2006 event, the mean energy is found to be 9.4 and 3.6 keV for ON and OFF periods respectively. For such high energies, model results show that I_{N_2} is directly proportional to the number flux of the precipitating electrons, with a conversion factor of 210 R(mW m^{-2})$^{-1}$. The flux from ASK varies from an average value of 3.3 mW m^{-2} during ON to 1.4 mW m^{-2} during OFF. For the 2007 event both the mean energy and energy flux are higher, 15 keV and 5.7 mW m^{-2} during ON and 6.0 keV and 2.8 mW m^{-2} during OFF. The reduction in energy between ON and OFF is about 62 % for 2006 and 61 % for 2007, which is very similar to the reduction in flux (about 57 % for 2006 and 55 % for 2007). The fits to the radar profiles in Fig. 3 are only an indication of the mean energies and fluxes, but the agreement with the optical estimates is good.

3.2 Brightness reduction below the background level

During several occasions of the pulsations, larger reductions, or dips, were seen at the time of the transition from ON to OFF. One such instance is displayed in the top panel of

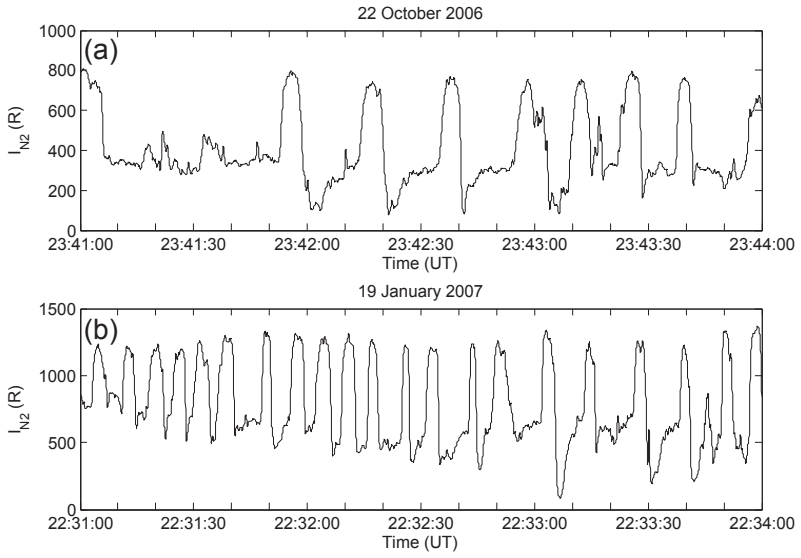

Figure 4. (a) Pc1 pulsations seen in I_{N_2} during 3 min on 22 October 2006. At the beginning of most OFF periods the emission brightness dips below the diffuse background emission. **(b)** I_{N_2} during 3 min on 19 January 2007. Dips are again seen just after the transition from ON to OFF.

Fig. 4, where the temporal evolution of I_{N_2} is plotted during an interval of regular Pc1 pulsations. The dips are seen in both I_{N_2} and I_O. The time interval is the same as in Fig. 2. The brightness has been background subtracted and averaged over a circle with a radius of 0.1°, pointed to the magnetic zenith. The pulsation period is approximately 21 s, and the ON periods show a fairly constant emission brightness level of 700 ± 80 R for I_{N_2} and 140 ± 10 R for I_O (not shown). At the beginning of each OFF period, the auroral brightness drops to a minimum for up to a second, after which the brightness builds up to a fairly constant OFF period brightness of 300 ± 40 R (I_{N_2}) and 90 ± 10 R (I_O). The N_2 brightness in the dip is about 100 R lower than the OFF period emissions, corresponding to a reduction of 70 %. The OFF periods last for approximately 15 s. The I_O emission is faint, which makes the data fairly noisy. The relative decrease in emission brightness in the dips is similar to that in I_{N_2}. The fact that the dips are seen in both emissions with a similar percentage of reduction indicates that the decrease is independent of the energy of the precipitation.

Dips were also detected during the 2007 event. The bottom panel in Fig. 4 shows 3 min of I_{N_2} from that event, where dips can be seen at the beginning of most OFF periods, but not for all of them. The depth is more varied, which could be affected by the more variable background level on this day. The largest reduction is 86 % below the average OFF brightness.

There is no spatial variation in the dips across the ASK 3° field of view (which corresponds to 5×5 km at 100 km altitude). Figure 5a shows the variation of I_{N_2} as measured within squares of 10 by 10 pixels, at 10 different locations across the field of view (Fig. 5b). Although there are some differences in brightness across the image, like the brighter emissions detected in the top left corner of the image at the beginning of the interval, the dips are noticeable in all 10 regions and are of equal depth.

The pulsation pattern experienced another type of dip 10 min before the data sequence with dips on 19 January 2007 where the reduction below the average OFF brightness level occurred just before the ON period rather than just after. The decrease in brightness leading up to the dip is slower than that of the dips seen just after ON. These dips can be seen in Fig. 6, showing 2 min of I_{N_2} data, where again the brightness has been background subtracted and averaged over a circle with a radius of 0.1°, pointed to the magnetic zenith. The dips are also seen in the I_O data. The pulsations cover the whole field of view in ASK, so that no structure is seen in the images at this time; the brightness variations are seen in the diffuse emissions.

3.3 Rise and fall times of pulsations

The rise and fall times were investigated for 219 pulsations that appeared during the two events, where the times were estimated using an automated fitting routine to each pulsation. The method is further described and demonstrated below. From the 22 October 2006 event there are 124 pulsations, and from 19 January 2007 there are 95 pulsations. The average rise time of the pulsations is 1.6 ± 1.0 s, and average fall time is somewhat shorter, 1.4 ± 0.9 s. The top panel of Fig. 7 shows the distribution of rise times for the pulsations, and the bottom panel shows the fall times. The data from the event in 2006 are plotted as dark blue, and the data from the event in 2007 are shown in light blue. Both rise and

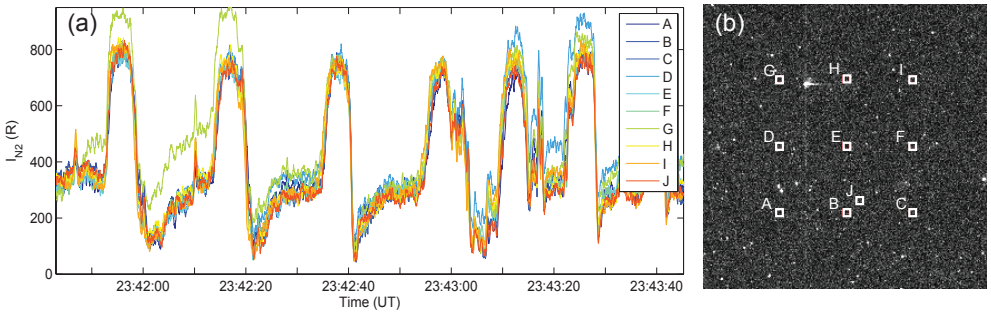

Figure 5. (a) N_2 emission brightness in 10 different locations across the ASK field of view. The locations where the brightness has been measured are shown in **(b)**. Very little variation in brightness is seen for the different measuring points, and the brightness dips at the beginning of the pulsation OFF period are equally distinguished in all locations.

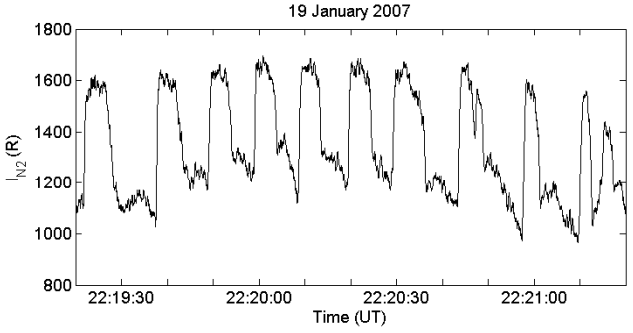

Figure 6. Dips have also been seen just before the ON period of pulsations, but often with a slow decrease in brightness to reach a minimum value, as is shown here in the I_{N_2} data.

fall times are slightly longer for the 2006 event (on average 1.8 and 1.4 s) compared with the 2007 event (on average 1.3 and 1.3 s). The shape of the distribution is also somewhat different for the two events, with the distribution for the 2007 data being positively skewed and the 2006 distribution being more symmetrical. If looking at the difference in rise and fall times for each pulse (shown in Fig. 8), a longer rise time than fall time happens for 60 % of the pulsations, whereas 37 % exhibit longer fall times.

The duration of the ON period of the pulsations ranges from 0.2 to 7.3 s, with an average duration of the ON period of 2.4 ± 1.0 s. The distribution is shown in Fig. 9, and the ON duration is in general longer for the 2006 event (2.6 s) compared with the 2007 event (2.2 s). Over the course of our events lasting a few hours, slower variations are seen in the background level, and the pulsations are superimposed on the varying background so that the difference between the brightness level during the ON and OFF periods is relatively constant for consecutive pulsations. For the data from the two events analysed here, the brightness increase above the background is on average 510 ± 220 R for I_{N_2}. The increase is on average lower (460 R compared with 550 R) during the 2007 event than the 2006 event. There is no found correlation ($r = 0.04$) between the duration of the ON period and the brightness enhancement of the pulsation for the studied events.

Most auroral pulsations in the data set show regular and symmetric rise and fall times of the emission brightness. In the data analysed in this study, we have detected a number of auroral pulses exhibiting a slower increase than decrease, but we have also seen the opposite case, where the fall time is significantly longer than the rise time. There are indications of a bump-on-tail feature for both rise and fall times in Fig. 7 at around 4 s. Similarly, in Fig. 8, the bump at about 2 s (and possibly also near −2) indicates that asymmetrical pulsations are common, where the difference between rise and fall time is near 2 s. Figure 10 shows four examples of asymmetric pulsations found in the data from 19 January 2007. Figure 10a and c are examples of a slower decrease, whereas Fig. 10b and d show pulsations with a slower increase in brightness. The horizontal red lines in the figures show the mean brightness level during ON and OFF and the tilted lines the linear fit to the increase and decrease. These fits have been used to estimate the duration of the rise and fall.

4 Discussion

We have presented auroral pulsation data captured with incoherent scatter radar and small field-of-view cameras at two different wavelengths, 673 nm for observations of the N_2 1PG band and 777.4 nm for observations of O emissions. Data are shown from two nights of pulsating aurora, 22 October 2006 and 19 January 2007. The two emissions have very different response curves to the energy of the precipitating electrons; the N_2 emissions are excited by both high and low energy of the precipitation, and the O emissions can be produced through two different processes, either direct excitation of O atoms or by dissociative excitation of O_2 through $O_2 + e^- \rightarrow O + O(3p) + e^-$ (see Fig. 1 of Lanchester et al., 2009). For large energies such as are typical for pulsating aurora, the contribution to O emissions measured in ASK3 is small, which leads to large uncertainties. In addition, the

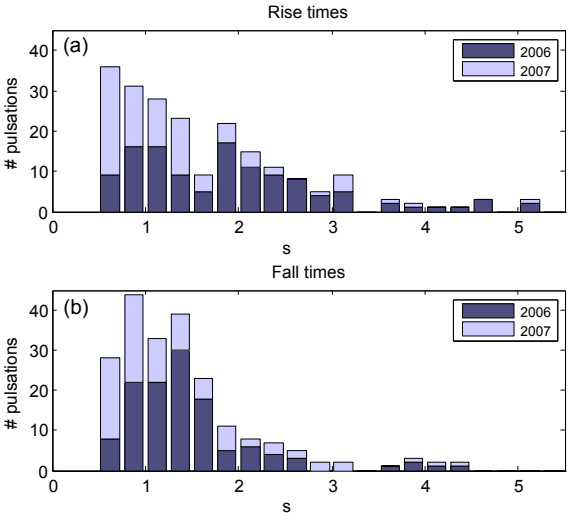

Figure 7. (a) Distribution of rise times for 219 pulsations detected during the two events. **(b)** Distribution of fall times for the same pulsations.

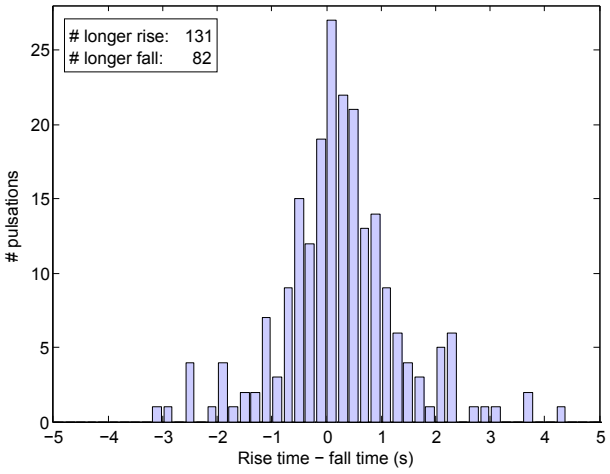

Figure 8. Distribution of the difference in rise and fall time for the pulsations.

optical ratio method to derive estimated energies is very sensitive to the background subtraction. Due to this, the relative changes in energy flux found from I_{N_2} are more reliable than estimating the energy change. Even so, the mean energy during ON and OFF periods for the two events is comparable with estimates obtained by fitting modelled electron density profiles to the measured profiles by EISCAT. The results are consistent with previous observations by rockets, where it was found that the ON pulsation corresponded to increased flux of electrons with energies above 5 keV (Sandahl et al., 1980). Studies have shown that dark filaments that can appear in diffuse aurora, so-called black aurora, are correlated with a slight reduction of energy and flux, but that the optical emissions are not reduced completely (e.g. Archer et al., 2011). The similarity between the energy and flux reductions observed in black aurora and those measured in these pulsating events suggests that a similar mechanism needs to be taken into account for both phenomena and that the black aurora appear as structures that are constantly in OFF mode.

The temporal resolution of the ASK data is 32 Hz, which is more than sufficient to detect any 3 ± 1 Hz modulations in the ON periods that are believed to be due to short whistler-mode elements within each chorus burst. However, no 3 Hz modulation is detected for the events discussed here. The derived energy of the precipitation fits with theories of chorus waves as a source mechanism, and it is possible that the 3 Hz modulation is not visible due to energy dispersion effects; however, it could also indicate that a different source mechanism is at play.

As shown in the data, the brightness levels at ON and OFF periods are fairly constant for consecutive pulses, with only slow variations over time, as if the precipitation is switching between two fixed source populations. Yamamoto (1988) also concluded from their observations that the background conditions vary very little during several cycles of pulsations. Davidson (1990) discussed the precipitating electrons as consisting of two different components: a steady diffuse component with an energy spectrum extending towards lower energies and a pulsating component caused by higher-energy flux electrons. The dominant source of electron precipitation causing diffuse aurora has been shown to be chorus waves (Thorne et al., 2010; Ni et al., 2016). Miyoshi et al. (2015) showed with observations of energy spectra and simulations that while lower band chorus waves can lie behind the main modulation of the electron precipitation, causing pulsating aurora, upper band chorus waves can produce a simultaneous, constant precipitation at about 1 keV. They furthermore argued that this is the source of the precipitation during the OFF period of pulsations. However, our observations, as well as earlier rocket observations by Sandahl et al. (1980), show that the energy of the background precipitation is much higher than this, of the order of several kilo-electronvolts, which suggests that upper band chorus waves alone are not responsible for the background emissions observed here. The high energies during both ON and OFF periods found here are a strong indication that the same mechanism is acting on both components, with some modulation. This is further supported by the observations of reductions in the background emission; it is clear that the process causing dips in the OFF brightness is connected with the ON period of the pulsations, or with the transition between ON and OFF. Therefore, the same mechanism should be considered when discussing the precipitation during both ON and OFF periods of pulsating aurora. The fact that the dip signatures are very similar over the whole ASK field of view indicates that it is not a localised spatial feature, but instead the dips are likely characteristic for the whole pulsating patch and signatures of a modification formed at the electron modulation source region.

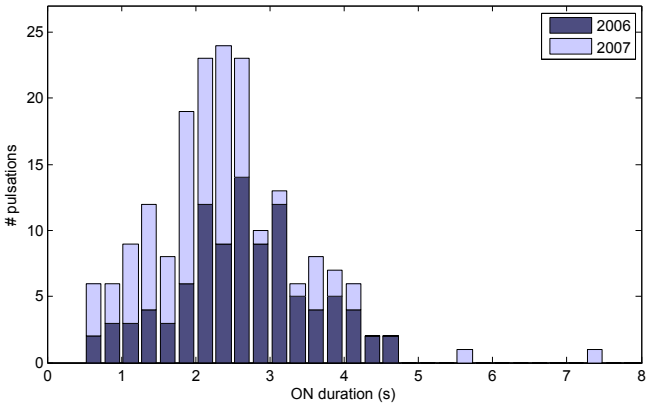

Figure 9. ON duration of each pulse for the two events. The pulsations during the 2006 event are on average longer than those during the 2007 event.

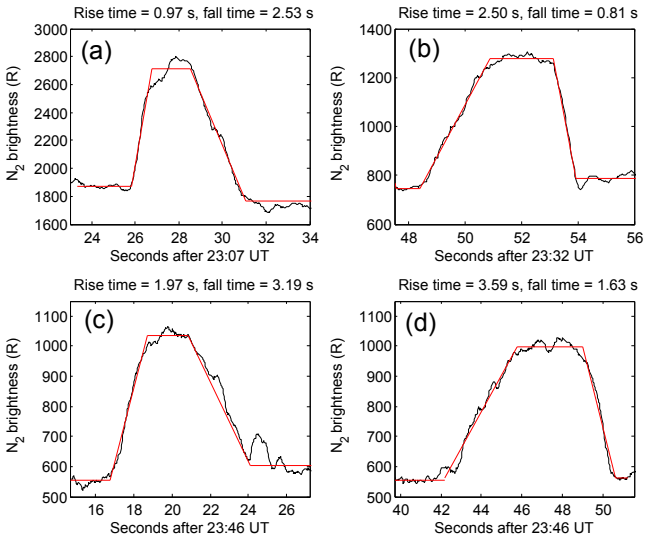

Figure 10. Auroral pulsations observed on 19 January 2007, with asymmetric appearance. In **(a, c)** the fall time of brightness is much longer than the rise time, and in **(b, d)** the opposite is true. The horizontal red lines show the mean brightness level and the sloped line shows the linear fit to the rise and fall used to estimate the time.

One strong candidate for explaining the pulsating pattern is the nonlinear relaxation oscillator model (Davidson, 1979, 1990), where wave growth results from anisotropy in the phase space distribution, causing stronger scattering into the loss cone. Since the timescales of the wave period and growth are much shorter than the electron bounce period, the loss cone gets filled and the anisotropy is reduced, which in turn reduces the amplitude of the waves. As the loss cone empties through precipitation of electrons to the ionosphere, the conditions for wave growth are reestablished. The dips in the background emission seen directly after the ON period of the pulsations could be the result of a complete drainage of the loss cone, which then slowly refills again. Occasionally the brightness also shows a slow decrease during the OFF period and a dip just before the build up to the ON period. These dips before ON were never observed in conjunction with the dips just after the ON period, and they are often not as sharp but have a longer fall time. It is not clear what could cause such slow decreases in the background level just before the ON period of the pulsations. One possibility is that they are related to variations in the local density. It has been suggested that the modulation of precipitation into pulses is due to flux tubes with enhanced cold plasma density, which act as a resonator for whistler waves (Demekhov and Trakhtengerts, 1994). Recent observations by THEMIS have also shown a strong correlation between whistler waves and density depletions (Li et al., 2011). Other studies based on observations with the Van Allen Probes in the magnetosphere suggest that excited ultra-low-frequency (ULF) waves are responsible for chorus wave modulation (Jaynes et al., 2015; Xia et al., 2016). It is possible that the ULF modulation of the electron density may affect the wave growth of different VLF wave modes differently, which could lead to lag times responsible for the dips. The central question of what causes the (quasi-) periodicity of pulsating aurora is thus still under debate.

The pulsations during both events exhibit a shorter average duration of the ON period compared to earlier similar statistical studies, where the duration distribution peaked at about 6 s (Humberset et al., 2016; Yamamoto, 1988). This could be attributed to the separation of rise time, ON time, and fall time in this study, where the average rise and fall time is more than a second each. If we include half the rise and fall times in the ON time, the average ON time is estimated at 3.9 s, which is closer to previous results but still significantly shorter. However, there is a non-negligible difference in duration time between the two events studied here, and in each of the previous studies the data also came from a few minutes or hours of continuous measurements from one specific event. It is therefore likely that the difference in duration period and similar characteristics are the result of different geophysical conditions associated with each event.

Occasionally the pulsations observed in our study exhibited an asymmetry in rise and fall times. Pulses with a slower rise time appeared as a few consecutive pulses, and the pulses with a slower fall time appeared for at most two pulsations at a time. The slow rise time is unlikely to be due to time-of-flight effects of electrons of varying energy since the rise time is much longer than realistic dispersion times, as observed with Reimei and modelled by Miyoshi et al. (2010), and also since the pulses of slower rise time are not seen for the majority of the pulses, which would then be the case. Samara and Michell (2010) also found auroral pulsations where the rise time was slower than the fall time. They attributed their observations to an increase in frequency of the chorus wave bursts, which they found to be correlated with the optical in-

tensity of the aurora. We speculate that a slower rise may be attributed to less efficient scattering into the loss cone where the interaction time of the waves and particles is extended in the relaxation oscillator model. This would also result in a slower increase of power spectral density of the chorus bursts that last a few seconds. The chorus bursts shown in Fig. 1c in Li et al. (2013) show variability in power spectral density for each burst, for example, with a burst with slower increase than decrease seen at 08:19:30 UT in their figure. Information on the variations of rise and fall times can likely be used to scrutinise the formation models of pulsating aurora.

Jaynes et al. (2013) reported a sawtooth appearance of the electron flux measured near the magnetic equator with a slower fall than rise and saw a similar slower fall in the corresponding auroral emissions. They speculated that the asymmetry was the result of the relaxation oscillator, where the longer fall time is due to diffusion of electrons at adjacent pitch angles during their bounce periods, which becomes less and less effective. A similar feature was also observed by Humberset et al. (2016). The main difference between the pulsations with longer fall times seen here and those reported by Jaynes et al. (2013) is the repetition rate; the sawtooth pattern covered many pulsation periods, whereas ASK only detected sporadic pulsations with a longer fall time. Even so, there is a faint bump in the fall time distribution at about 4 s in Fig. 7, which indicates that there must be a causative physical phenomenon giving rise to similar fall times. This signature is not as clear for the rise times. Figure 8 shows too that asymmetric pulsations frequently occur during the events studied here, where either rise time or fall time is about 2 s longer than the other.

5 Conclusions

We report here on observations from high-speed imaging and incoherent scatter radar of two pulsating aurora events. Both events took place during the recovery phase of a substorm, just after magnetic midnight. The high-resolution data made it possible to study the detailed temporal variations in energy, flux, and brightness during the events. The key results are that

1. the energy and flux were both reduced by a factor of about 60 % during OFF compared with ON periods of the pulsations for the two events. This result implies that the number flux of higher-energy electrons is reduced in the OFF intervals; however, energies remain at a few kilo-electronvolts during the OFF intervals, which has implications for formation theories. No 3 Hz modulations were detected in the optical data.

2. several brightness reductions below the average OFF brightness level occurred on both nights, where the optical intensity dropped sharply just after the ON period of the pulsations and then rose quickly to the background level. An instance of several dips occurring just before the ON period was also noted. For these dips, the fall time is longer. The dips could be attributed to reaching isotropy during the relaxation oscillator theory, so that wave–particle interactions are suppressed. It is of importance to note that the dips in the background level are always correlated with the ON phase of the pulsations (either just before or after), which indicates an interaction between the background population and the pulsating population.

3. the rise and fall times of auroral pulsations were investigated and were found to be on average 1.6 ± 1.0 and 1.4 ± 0.9 s. The average ON time is 2.4 ± 1.0 s. Several asymmetric edges of the pulsations are observed in the data set, where either the rise or fall time is about 4 s instead of the typical 0.5–2 s. A longer rise time is observed to be more common than a longer fall time. The asymmetric pulses with longer fall time appear sporadically, whereas pulses with longer rise time often occur for a few pulses at a time. To fully understand what could cause such asymmetry in only short intervals of longer pulsation trains, external factors affecting the diffusion of electrons into the loss cone need to be considered.

Data availability. Radar data is available through the EISCAT data portal: 22 October 2006 data can be downloaded at https://www.eiscat.se/schedule/tape2.cgi?date=20061022&exp=arc1u_cp1_1.00_SP&dl=1, and 19 January 2007 data is found at https://www.eiscat.se/schedule/tape2.cgi?date=20070119&exp=arc1u_cp1_1.00_SP&dl=. ASK keograms for the two events and videos of two 3 min intervals containing the brightness dips are available at http://dx.doi.org/10.5258/SOTON/D0042 (Dahlgren et al., 2017). The raw ASK data are stored on magnetic tapes and are made available upon request.

Competing interests. The authors declare that they have no conflict of interest.

Acknowledgements. ASK has been funded by PPARC, NERC, and STFC of the United Kingdom and the Swedish Research Council. Hanna Dahlgren is supported by the Swedish Research Council under grant 350-2012-6591. Daniel Whiter is supported by NERC grant NE/N004051/1. EISCAT is an international association supported by research organisations in China (CRIRP), Finland (SA), Japan (NIPR and STEL), Norway (NFR), Sweden (VR), and the United Kingdom (NERC).

The topical editor, K. Hosokawa, thanks the two anonymous referees for help in evaluating this paper.

References

Archer, J., Dahlgren, H., Ivchenko, N., Lanchester, B. S., and Marklund, G. T.: Dynamics and characteristics of black aurora as observed by high-resolution ground-based imagers and radar, Int. J. Remote Sens., 32, 2973–2985, doi:10.1080/01431161.2010.541517, 2011.

Bryant, D. A., Smith, M. J., and Courtier, G. M.: Distant modulation of electron intensity during the expansion phase of an auroral substorm, Planet. Space Sci., 23, 867–878, doi:10.1016/0032-0633(75)90022-7, 1975.

Coroniti, F. V. and Kennel, C. F.: Electron precipitation pulsations, J. Geophys. Res., 75, 1279–1289, doi:10.1029/JA075i007p01279, 1970.

Dahlgren, H., Ivchenko, N., Sullivan, J., Lanchester, B. S., Marklund, G., and Whiter, D.: Morphology and dynamics of aurora at fine scale: first results from the ASK instrument, Ann. Geophys., 26, 1041–1048, doi:10.5194/angeo-26-1041-2008, 2008.

Dahlgren, H., Lanchester, B. S., Ivchenko, N., and Whiter, D. K.: ASK keograms and videos for study on variations in energy, flux and brightness of pulsating aurora measured at high time resolution, doi:10.5258/SOTON/D0042, University of Southampton, 2017.

Davidson, G.: Self-modulated VLF wave-electron interactions in the magnetosphere: A cause of auroral pulsations, J. Geophys. Res.-Space, 84, 6517–6523, doi:10.1029/JA084iA11p06517, 1979.

Davidson, G. T.: Pitch-angle diffusion and the origin of temporal and spatial structures in morningside aurorae, Space Sci. Rev., 53, 45–82, doi:10.1007/BF00217428, 1990.

Demekhov, A. G. and Trakhtengerts, V. Y.: A mechanism of formation of pulsating aurorae, J. Geophys. Res.-Space, 99, 5831–5841, doi:10.1029/93JA01804, 1994.

Horne, R. B., Thorne, R. M., Meredith, N. P., and Anderson, R. R.: Diffuse auroral electron scattering by electron cyclotron harmonic and whistler mode waves during an isolated substorm, J. Geophys. Res.-Space, 108, 1290, doi:10.1029/2002JA009736, 2003.

Humberset, B. K., Gjerloev, J. W., Samara, M., Michell, R. G., and Mann, I. R.: Temporal characteristics and energy deposition of pulsating auroral patches, J. Geophys. Res.-Space, 121, 7087–7107, doi:10.1002/2016JA022921, 2016.

Jaynes, A. N., Lessard, M. R., Rodriguez, J. V., Donovan, E., Loto'aniu, T. M., and Rychert, K.: Pulsating auroral electron flux modulations in the equatorial magnetosphere, J. Geophys. Res.-Space, 118, 4884–4894, doi:10.1002/jgra.50434, 2013.

Jaynes, A. N., Lessard, M. R., Takahashi, K., Ali, A. F., Malaspina, D. M., Michell, R. G., Spanswick, E. L., Baker, D. N., Blake, J. B., Cully, C., Donovan, E. F., Kletzing, C. A., Reeves, G. D., Samara, M., Spence, H. E., and Wygant, J. R.: Correlated Pc4–5 ULF waves, whistler-mode chorus, and pulsating aurora observed by the Van Allen Probes and ground-based systems, J. Geophys. Res.-Space, 120, 8749–8761, doi:10.1002/2015JA021380, 2015.

Johnstone, A. D.: Pulsating aurora, Nature, 274, 119–126, doi:10.1038/274119a0, 1978.

Johnstone, A. D.: The mechanism of pulsating aurora, Ann. Geophys., 1, 397–410, 1983.

Jones, S. L., Lessard, M. R., Rychert, K., Spanswick, E., Donovan, E., and Jaynes, A. N.: Persistent, widespread pulsating aurora: A case study, J. Geophys. Res.-Space, 118, 2998–3006, doi:10.1002/jgra.50301, 2013.

Lanchester, B. and Gustavsson, B.: Imaging of Aurora to Estimate the Energy and Flux of Electron Precipitation, Am. Geophys. Un., 171–182, doi:10.1029/2011GM001161, 2013.

Lanchester, B. S., Rees, M. H., Sedgemore, K. J. F., Palmer, J. R., Frey, H. U., and Kaila, K. U.: Ionospheric response to variable electric fields in small-scale auroral structures, Ann. Geophys., 16, 1343–1354, doi:10.1007/s00585-998-1343-8, 1998.

Lessard, M. R.: A Review of Pulsating Aurora, Am. Geophys. Un., 55–68, doi:10.1029/2011GM001187, 2013.

Li, W., Bortnik, J., Thorne, R. M., Nishimura, Y., Angelopoulos, V., and Chen, L.: Modulation of whistler mode chorus waves: 2. Role of density variations, J. Geophys. Res.-Space, 116, a06206, doi:10.1029/2010JA016313, 2011.

Li, W., Bortnik, J., Nishimura, Y., Thorne, R. M., and Angelopoulos, V.: The Origin of Pulsating Aurora: Modulated Whistler Mode Chorus Waves, Am. Geophys. Un., 379–388, doi:10.1029/2011GM001164, 2013.

McEwen, D. J., Yee, E., Whalen, B. A., and Yau, A. W.: Electron energy measurements in pulsating auroras, Can. J. Phys., 59, 1106–1115, doi:10.1139/p81-146, 1981.

Meredith, N. P., Horne, R. B., Thorne, R. M., and Anderson, R. R.: Survey of upper band chorus and ECH waves: Implications for the diffuse aurora, J. Geophys. Res.-Space, 114, a07218, doi:10.1029/2009JA014230, 2009.

Miyoshi, Y., Katoh, Y., Nishiyama, T., Sakanoi, T., Asamura, K., and Hirahara, M.: Time of flight analysis of pulsating aurora electrons, considering wave-particle interactions with propagating whistler mode waves, J. Geophys. Res.-Space, 115, a10312, doi:10.1029/2009JA015127, 2010.

Miyoshi, Y., Saito, S., Seki, K., Nishiyama, T., Kataoka, R., Asamura, K., Katoh, Y., Ebihara, Y., Sakanoi, T., Hirahara, M., Oyama, S., Kurita, S., and Santolik, O.: Relation between fine structure of energy spectra for pulsating aurora electrons and frequency spectra of whistler mode chorus waves, J. Geophys. Res.-Space, 120, 7728–7736, doi:10.1002/2015JA021562, 2015.

Nakajima, A., Shiokawa, K., Sakaguchi, K., Miyoshi, Y., Lee, S., Angelopoulos, V., Le Contel, O., McFadden, J. P., Bonnell, J. W., Fornacon, K.-H., and Donovan, E.: Electron and wave characteristics observed by the THEMIS satellites near the magnetic equator during a pulsating aurora, J. Geophys. Res.-Space, 117, a03219, doi:10.1029/2011JA017066, 2012.

Ni, B., Thorne, R. M., Zhang, X., Bortnik, J., Pu, Z., Xie, L., Hu, Z.-J., Han, D., Shi, R., Zhou, C., and Gu, X.: Origins of the Earth's Diffuse Auroral Precipitation, Space Sci. Rev., 200, 205–259, doi:10.1007/s11214-016-0234-7, 2016.

Nishimura, Y., Bortnik, J., Li, W., Thorne, R. M., Lyons, L. R., Angelopoulos, V., Mende, S. B., Bonnell, J. W., Le Contel, O., Cully, C., Ergun, R., and Auster, U.: Identifying the Driver of Pulsating Aurora, Science, 330, 81–84, doi:10.1126/science.1193186, 2010.

Nishimura, Y., Bortnik, J., Li, W., Thorne, R. M., Chen, L., Lyons, L. R., Angelopoulos, V., Mende, S. B., Bonnell, J., Le Contel, O., Cully, C., Ergun, R., and Auster, U.: Multievent study of the correlation between pulsating aurora and whistler mode chorus emissions, J. Geophys. Res.-Space, 116, a11221, doi:10.1029/2011JA016876, 2011.

Nygrén, T., Kaila, K. U., Huuskonen, A., and Turunen, T.: Determination of E region effective recombination coefficient using impulsive precipitation events, Geophys. Res. Lett., 19, 445–448, doi:10.1029/92GL00118, 1992.

Palmer, J. R.: Plasma density variations in aurora, PhD thesis, University of Southampton, Southampton, UK, 1995.

Royrvik, O. and Davis, T. N.: Pulsating aurora: Local and global morphology, J. Geophys. Res., 82, 4720–4740, doi:10.1029/JA082i029p04720, 1977.

Samara, M. and Michell, R. G.: Ground-based observations of diffuse auroral frequencies in the context of whistler mode chorus, J. Geophys. Res.-Space, 115, a00F18, doi:10.1029/2009JA014852, 2010.

Samara, M., Michell, R. G., Asamura, K., Hirahara, M., Hampton, D. L., and Stenbaek-Nielsen, H. C.: Ground-based observations of diffuse auroral structures in conjunction with Reimei measurements, Ann. Geophys., 28, 873–881, doi:10.5194/angeo-28-873-2010, 2010.

Sandahl, I., Eliasson, L., and Lundin, R.: Rocket observations of precipitating electrons over a pulsating aurora, Geophys. Res. Lett., 7, 309–312, doi:10.1029/GL007i005p00309, 1980.

Sato, N., Wright, D. M., Carlson, C. W., Ebihara, Y., Sato, M., Saemundsson, T., Milan, S. E., and Lester, M.: Generation region of pulsating aurora obtained simultaneously by the FAST satellite and a Syowa-Iceland conjugate pair of observatories, J. Geophys. Res.-Space, 109, a10201, doi:10.1029/2004JA010419, 2004.

Stenbaek-Nielsen, H. C.: Pulsating aurora: The importance of the ionosphere, Geophys. Res. Lett., 7, 353–356, doi:10.1029/GL007i005p00353, 1980.

Thorne, R. M., Ni, B., Tao, X., Horne, R. B., and Meredith, N. P.: Scattering by chorus waves as the dominant cause of diffuse auroral precipitation, Nature, 467, 943–946, doi:10.1038/nature09467, 2010.

Trakhtengerts, V. Y.: A generation mechanism for chorus emission, Ann. Geophys., 17, 95–100, doi:10.1007/s00585-999-0095-4, 1999.

Xia, Z., Chen, L., Dai, L., Claudepierre, S. G., Chan, A. A., Soto-Chavez, A. R., and Reeves, G. D.: Modulation of chorus intensity by ULF waves deep in the inner magnetosphere, Geophys. Res. Lett., 43, 9444–9452, doi:10.1002/2016GL070280, 2016.

Yamamoto, T.: On the temporal fluctuations of pulsating auroral luminosity, J. Geophys. Res.-Space, 93, 897–911, doi:10.1029/JA093iA02p00897, 1988.